Published in final edited form as:
J Comp Neurol. 2007 October 10; 504(5): 499–507.

Analysis of Connexin Subunits Required for the Survival of Vestibular Hair Cells

YAN QU[1,2], **WENXUE TANG**[1], **IAN DAHLKE**[1], **DALIAN DING**[4], **RICHARD SALVI**[4], **GORAN SÖHL**[5], **KLAUS WILLECKE**[5], **PING CHEN**[1,3], and **XI LIN**[1,3,*]

1*Department of Otolaryngology, Emory University School of Medicine, Atlanta, Georgia 30322-3030*

2*Department of ENT, Third Hospital of Hebei Medical University, Shijiazhuang, Hebei, People's Republic of China 050051*

3*Department of Cell Biology, Emory University School of Medicine, Atlanta, Georgia 30322-3030*

4*Center for Hearing & Deafness, University of Buffalo, Buffalo, New York 14214*

5*Institute of Genetics, University of Bonn, 53117 Bonn, Germany*

Abstract

Mutations in connexin (Cx) genes are responsible for a large proportion of human inherited prelingual deafness cases. The most commonly found human Cx mutations are either Cx26 or Cx30 deletions. Histological observations made in the organ of Corti of homozygous Cx26 and Cx30 gene knockout mice show that cochlear hair cells degenerate after the onset of hearing. However, it is unclear whether vestibular hair cells undergo similar degeneration in connexin knockout mice. To address this question, we first examined expression patterns of Cx26 and Cx30 in the saccule, utricle, and ampulla by immunolabeling. In wild-type mice, Cx26 and Cx30 immunoreactivity was found extensively in vestibular supporting cells and connective tissue cells, and the two Cxs were co-localized in most gap junction (GJ) plaques. Targeted deletion of the Cx30 gene, which caused little change in Cx26 expression pattern, resulted in a significant and age-related loss of vestibular hair cells only in the saccule. dUTP nick end labeling (TUNEL) staining also revealed on-going apoptosis specifically in saccular hair cells of $Cx30^{-/-}$ mice. These results indicated that hair cell survival in the utricle and ampulae does not require Cx30. Importantly, over-expressing the Cx26 gene from a modified bacterial artificial chromosome in the $Cx30^{-/-}$ background rescued the saccular hair cells. These results suggest that it is the reduction in the total amount of GJs rather than the specific loss of Cx30 that underlies saccular hair cell death in $Cx30^{-/-}$ mice. Hybrid GJs co-assembled from Cx26 and Cx30 were not essential for the survival of saccular hair cells.

Indexing terms

hair cell degeneration; vestibular sensory organs; saccule; connexin; gap junction; vestibular adaptation; congenital hearing loss

Gap junctions (GJ) are the only known intercellular membrane channels that provide direct connections between cells for the exchange of intracellular biochemical and electrochemical signals. A family of membrane proteins named connexins (Cxs) forms the building blocks of GJs. Six compatible Cx subunits assemble together to form GJ hemichannel (connexon), and 12 of them produce a whole GJ channel. GJs have been observed among various types of cells

*Correspondence to: Xi Lin, Ph.D., Departments of Otolaryngology and Cell Biology, Emory University School of Medicine, 615 Michael Street, Atlanta, GA 30322. E-mail: xlin2@emory.edu.

in both the cochlear and vestibular systems by direct observations made at the electron microscopy level (Forge et al., 2003; Mulroy et al., 1993). Immunohistochemcial labeling studies further demonstrated that Cx26 and Cx30 are the two major subtypes of Cxs in the cochlea (Ahmad et al., 2003; Forge et al., 2003; Lautermann et al., 1999).

In the vestibular sensory organs immunolabeling revealed extensive Cx26 expression in both sensory and nonsensory epithelia (Kikuchi et al., 1994). Cx30 expression was also identified (Forge et al., 2003). The functional importance of GJs in hearing was revealed by genetic studies showing that a large portion of hereditary nonsyndromic hearing loss cases (~50%) is linked to mutations in the Cx26 (Gerido and White, 2004) and Cx30 (del Castillo et al., 2002a) genes. Previous investigations demonstrated that Cx26 and Cx30 are major Cx subunits expressed by the cochlear supporting cells (e.g., Hensen, Claudius, Deiters', interdental, and root cells) and connective tissue cells (e.g., stria basal cells, fibrocytes in the spiral limbus and spiral ligament; Kikuchi et al., 1994; Lautermann et al., 1999; Ahmad et al., 2003; Forge et al., 2003;). In the cochlea, Cx26 and Cx30 are co-assembled to form most of the GJ plaques (Ahmad et al., 2003; Forge et al., 2003; Sun et al., 2005). These hybrid GJs form a GJ-connected intercellular membrane channel system, making it possible for ions, nutrients, and signaling molecules to move intercellularly by passive diffusion among various types of supporting cells and cochlear connective tissue cells.

Fibrocytes in the connective tissues of the vestibular system are connected extensively by GJs (Kikuchi et al., 1994); however, it is not clear whether hybrid Cx26 and Cx30 GJs are extensively present in vestibular supporting cells and connective tissue cells. Furthermore, the functional requirement of Cx subunits for the survival of vestibular hair cells has not yet been examined. To address these questions, we first investigated the patterns of Cx30 and Cx26 expression in the three vestibular sensory organs by using a co-immunolabeling protocol performed with semithin sections (~0.5 μm). To investigate the role of Cx30 on the survival of vestibular hair cells, we compared the morphology of hair cell bodies and bundles in the three vestibular sensory organs of wild-type (WT) and $Cx30^{-/-}$ mice. Results revealed degeneration of hair cells exclusively in the saccule, but not in the ampulae and utricle, of $Cx30^{-/-}$ mice. dUTP nick end labeling (TUNEL) staining identified cells in the sacculus dying by apoptosis.

To differentiate whether the hair cell death was caused by a lack of hybrid GJs consisting of Cx26 and Cx30 or simply a reduction in total Cx protein expression (gene dosage effect), we overexpressed Cx26 by transgenic expression from a modified bacterial artificial chromosome (BAC) in the $Cx30^{-/-}$ background. Saccular hair cells were rescued by increasing the Cx26 gene dosage, presumably restoring the required amount of GJs needed for normal saccular functions. These results suggested that hybrid GJs co-assembled from Cx26 and Cx30 were not required for saccular hair cell survival and that a reduction in the total amount of functional GJs in Cx30 knockout mice apparently underlies the saccular hair cell death observed in the $Cx30^{-/-}$ mice.

MATERIALS AND METHODS

Morphological examinations

Animals used in this study were WT (strain C57), $Cx30^{-/-}$ mice (Teubner et al., 2003), and hearing rescued mice (BAC^{Cx26};$Cx30^{-/-}$ mice; Ahmad et al., 2007). The two genetically modified strains of mice used in this study ($Cx30^{-/-}$ and BAC^{Cx26};$Cx30^{-/-}$) were extensively characterized previously (Teubner et al., 2003; Ahmad et al., 2007). Ages of mice were from postnatal day 17 (P17) to 1 year. Age-matched mice were used for comparison of morphological changes among WT, $Cx30^{-/-}$ mice and BAC^{Cx26};$Cx30^{-/-}$ mice. At least eight

animals were used in each group. The animal use protocol was approved by the Emory Institutional Animal Care and Use Committee.

Mice were deeply anesthetized with xylazine (i.p., 100 mg/kg) and ketamine (i.p., 30 mg/kg). Animals were cardiac perfused with 0.1 M phosphate-buffered saline (PBS) followed by paraformaldehyde (4%, in 0.1 M PBS). The temporal bones were immediately removed, and the cochlear and vestibular portions were dissected out and postfixed in 4% paraformaldehyde for another 24 hours at 4°C. Samples were decalcified for 72 hours in ethylendiaminetetraacetate (EDTA) solution (0.35 M, pH 7.4). Decalcified samples were washed with PBS (2X for 30 minutes) and cryoprotected by immersion in 15% (for 20 minutes) and 20% (overnight) sucrose solution consecutively. Samples were embedded in OCT compound (Sakura Finetechnical, Tokyo, Japan) and sectioned in a direction parallel to the modiolus. Conventional sections were cut at a thickness of 8 μm by using a cryostat (Leica CM1850, Nussloch, Germany). Semithin cochlear sections (0.5 μm) were cut with an ultramicrotome (Leica-ultracut UCT, Leica Microsystems, Bannockburn, IL) usually used for preparing electron microscopy samples. The cryochamber on the ultramicrotome was cooled to −60°C before sectioning started, and the cutting head of ultramicrotome was cooled to −120° C when samples were sectioned. Procedures for preparing whole-mount cochlear and vestibular samples were described previously (Ahmad et al., 2007).

Immumofluorescent and TUNEL labeling protocols

Whole-mount or sectioned tissue samples were permeabilized with Triton (0.1% in PBS, pH 7.4) for 30 minutes. Nonspecific labeling was blocked with 10% goat serum in PBS at room temperature for 1 hour. Polyclonal antibodies against Cx26 and Cx30 were purchased from Invitrogen (Carlsbad, CA; catalog numbers 71-0500 [lot#5039349] and 71-2200 [lot#60706423], respectively). These Cx antibodies were raised in either rabbit or mouse by using synthetic peptides as antigens. The Cx26 antigenic peptide sequence was selected from the unique sequence in the cytoplasmic loop of the protein, which was RRHEKKRKFMKGEIK. The Cx30 antigenic peptide sequence was selected in the C-terminal unique to the Cx30, which was SKRTQAQRNHPNHALKESKQNEMNELISDSGQNAITSFPS. Western blot characterization and controls for the two antibodies were published previously. Both antibodies recognized a single band on Western blots at the expected molecular weights (Fig. 3 of Ahmad et al., 2007). Cx30 and Cx26 immunoreactivity disappeared in $Cx30^{-/-}$ mice (Ahmad et al., 2007) and conditional $Cx26^{-/-}$ mice (unpublished data) respectively. These data confirm that the binding of the two antibodies was specific to their intended target proteins.

An antibody against myosin 7a was used to label the cochlear and vestibular hair cells. This antibody was a gift from Dr. Tama Hasson's lab. The antibody was affinity purified from rabbit by using an antigen of human myosin 7a tail (amino acids 880–1,070). The sequence of the antigenic peptide was LRKEMSAKKAKEEAERKHQERLAQLAREDAERELKEKEAARRKKELLEQMERAR HEPVNHSDMVDKMFGFLGTSGGLPGQEGQAPSGFEDLERGRREMVEEDLDAALPL PDEDEEDLSEYKFAKFAATYFQGTTTHSYTRRPLKQPLLYHDDEGDQLAALAVWIT ILRFMGDLPEPKYHTAMSDGSEKIPV. Western blots showed a single band at the expected molecular weight, and immunolabeling demonstrated that this antibody specifically labeled hair cells (Hasson et al., 1997). The stock solution was diluted at 1:200, and samples were incubated at 4°C overnight. Fluorescein isothiocyanate (FITC)-conjugated secondary antibodies (Jackson ImmunoResearch, West Grove, PA) were used to visualize the primary antibody (1:800 dilution, 1 hour incubation at room temperature). Hair bundles were labeled by rhodamine-conjugated phalloidin (dilution 1:1,000; Invitrogen; catalog number R415, lot number 43166A) for 20 minutes at room temperature. Phalloidin is a toxin that binds

specifically to F-actin, which is extensively expressed by the stereocilia of hair cells (Hasson et al., 1997). Most sections were also counterstained with 4′,6-diamidino-2-phenylindole (DAPI; Molecular Probes, Eugene, OR, catalog number D1306) to reveal the location of cell nuclei.

Processed samples were mounted in antifade solution (Fluoromount-G, Electron Microscopy Sciences, Hatfield, PA) and examined by using a confocal microscope (Zeiss LSM, Carl Zeiss, Thornwood, New York). Apoptotic cells were detected by using an in situ cell death detection kit (Roche, Mannheim, Germany). Apoptotic cleavage of genomic DNA was identified by terminal deoxynucleotidyl transferase (TdT)-mediated TUNEL) by following the manufacturer's instructions. Positive controls for apoptosis were obtained by treating cochlear sections with *DNase* I.

The percentage of Cx26 and Cx30 co-localization was obtained by counting the number of yellow pixels and dividing it by the total number of red and green pixels present in the co-immunolabeled samples (Fig. 2). Yellow pixels represent the area co-labeled by both antibodies. The images were analyzed by using image analysis software that is customer programmed with Labview (version 6i, National Instruments, Austin, TX). Photomicrographs were reorganized and edited in Photoshop (version CS2, Adobe Systems, San Jose, CA). Images were not manipulated except for slight adjustments of contrast and brightness to match different panels in the same figure.

RESULTS

Patterns of Cx30 immunoreactivity in the three vestibular sensory organs showed that most Cx30- and Cx26-positive GJ plaques were colocalized

Immunofluorescent labeling from the cristae ampullaris (Fig. 1, top row), saccule (Fig. 1, middle row), and utricle (Fig. 1, bottom) of WT mice demonstrated extensive immunoreactivity to both Cx26 and Cx30 in all three vestibular sensory regions. The punctate staining patterns (examples indicated by arrows in the panels of the two bottom rows), presumably representing clusters of GJ plaques around DAPI-labeled cell nuclei (Figs. 1, 2, in blue), were not as clearly observable if regular cryosections with a thickness of 8 μm were used in immunolabeling due to the high density of Cx26 and Cx30 immunoreactivity. We therefore used semithin cyrosections in our studies. Punctate Cx30 (colored green) and Cx26 (colored red) immunopositive spots were observed in supporting cells in all three sensory epithelia and regions beneath it (Figs. 1, 2). Thickness of the sensory epithelia is indicated by double-headed arrows in Figure 1A, D, and G. Overlapping patterns of the distinct Cx26 and Cx30 puncta were revealed more clearly in enlarged pictures for the boxed areas in Figure 2C, F, and I.

When we compared the density of connexin-positive puncta co-labeled by Cx26 and Cx30, we found that the subsensory epithelium region has a much higher density than the puncta in the sensory cell region (comparing Fig. 2A–C with D–F). Subepithelial cells, some of which are presumably fibrocytes, were strongly immunolabeled (Figs. 1, 2,D–F). Double immunolabeling with a hair cell-specific antibody (myosin 7) and Cx antibodies showed that vestibular hair cells were not labeled by Cx26 and Cx30 antibodies (data not shown). These results are consistent with previous reports about Cx26 and Cx30 expression patterns in the vestibular sensory regions (Kikuchi et al., 1994; Forge et al., 2003). In addition, our data demonstrated the extensive co-localization of Cx26 and Cx30 immunoreactivity in all three vestibular sensory regions. Most labeled puncta in the sensory epithelium (97 ± 11%, n = 10) and subsensory epithelium (91 ± 12%, n = 10) were double labeled by both Cx26 and Cx30 (Fig. 2, punctae colored yellow). The co-localization of Cx26 and Cx30 appeared to include all types of cells in both sensory and connective tissue regions, which indicated the presence of a continuum of hybrid (heteromeric and/or heterotypic) GJ channels coupling cells in

connective tissues in both the vestibular and cochlear sensory organs (Kikuchi et al., 1994; Sun et al., 2005).

In the cochlea of $Cx30^{-/-}$ mice, our previous report confirmed that Cx30 gene transcription and translation were both absent (Teubner et al., 2003; Ahmad et al., 2007). In this study we further confirmed that immunolabeling of Cx30 was negative in all three vestibular sensory regions (Fig. 3A–C). The patterns of Cx26 immunoreactivity in the ampulla (Fig. 3D), saccule (Fig. 3E), and utricle (Fig. 3F) of $Cx30^{-/-}$ mice, however, were unaltered compared with the WT animals. These results suggested that the absence of the Cx30 gene did not appreciably affect the expression pattern of Cx26 in the vestibular end organs. It is known from both in vivo and in vitro studies that Cx26 can self-assemble to form homomeric GJs (Thonnissen et al., 2002). Therefore, it is likely that homomeric Cx26 GJs are present in the vestibular sensory organs of $Cx30^{-/-}$ mice, although the total amount of GJ channels might be reduced compared with WT mice due to an overall reduction in gene dosage.

Cx30 gene knockout results in loss of saccular hair cells; increased expression of Cx26 rescued saccular hair cells in $Cx30^{-/-}$ mice

The effects of inactivating the Cx30 gene on the morphology of vestibular hair cell bundles were examined by immunolabeling with fluorescently conjugated phalloidin, and the results were observed with a confocal microscope. Comparison of vestibular stereocilia bundles of WT (Fig. 4, left column) and $Cx30^{-/-}$ (Fig. 4, middle column) mice revealed a nearly total loss of hair bundles specifically in the saccule of the mutant mice (n = 12, Fig. 4H). In contrast, patterns and densities of hair bundles in both ampulla (Fig. 4B) and utricle (Fig. 4E) were not obviously affected by the absence of the Cx30 gene. As a positive control, we found substantial inner and outer hair cell losses in both basal (Fig. 5A) and apical (Fig. 5B) turns of these $Cx30^{-/-}$ mice that demonstrated abnormal hair bundle morphology specifically in the saccule. Double immunolabeling of hair cell soma with myosin7 antibody (colored green) and stereocilia with Cy3-phalloidin antibody (colored magenta) revealed that saccular hair bundles were present in early postnatal animals (P4, Fig. 6A, example given by an arrow).

These results suggested that, similar to cochlear hair cells, lack of the Cx30 gene did not significantly affect the early development of vestibular hair cells. Most of the saccular hair cell bundles were lost at P14 (Fig. 6B), and degeneration of hair cell soma followed the loss of hair bundles. At postnatal day 14 (Fig. 6B), when most saccular hair bundles were already missing in $Cx30^{-/-}$ mice, most soma of hair cells were still observed and arranged in a normal pattern (Fig. 6B). The cell body of saccular hair cells, however, gradually disappeared and became disorganized as the animals matured. The time courses of saccular hair loss varied greatly among animals. In general, some hair cell bodies are still present 30 days after birth (Fig. 6C), and most hair cell soma in the saccule have died by about 6 months. The saccular hair cell loss appeared to be permanent, as we never observed hair bundle reappearance in $Cx30^{-/-}$ mice, as has been reported in some other species (Gale et al., 2002).

In addition to the morphological examinations, we performed TUNEL staining to capture on-going apoptotic cells in the vestibular sensory organs (Fig. 7). The soma of the hair cells was labeled by using an antibody against myosin7 (green immunolabeling in Fig. 7). The TUNEL-positive cells (colored magenta) were specifically found in both the hair cell and supporting cell regions of the saccule (examples given by arrows in Fig. 7C). Cells in both utricle (Fig. 7A) and ampulla (Fig. 7B) were TUNEL negative. These results were consistent with the findings observed from the pattern of hair cell loss in the vestibular sensory organs (Fig. 4).

Co-localization of Cx26 and Cx30 in most vestibular GJ plaques (Figs. 1, 2) suggested that they are co-assembled from Cx26 and Cx30. In addition, it is known that Cx26 can self-assemble to form homomeric GJs (Thonnissen et al., 2002). Therefore, saccular hair cell death

could be due to either a reduction of overall GJ quantity or the loss of hybrid Cx26 and Cx30 GJs that are irreplaceable by homomeric Cx26 GJs. To differentiate among these two molecular mechanisms, we repeated our morphology examinations by using BAC transgenic mice (BAC^{Cx26};$Cx30^{-/-}$ mice), in which a modified BAC harboring extra copies of Cx26 gene was transgenically expressed in the $Cx30^{-/-}$ background (Ahmad et al., 2007).

Our data showed that overexpressing Cx26 restored the normal morphology of saccular hair cells (n = 10, Fig. 4C,F,I). TUNEL staining also failed to find apoptotic saccular hair cells in these rescued mice (data not shown). The rescue effect was present in animals at least 6 months after birth, which are the oldest mice we have observed so far. These results indicate that a reduction in the gene dosage in $Cx30^{-/-}$ mice for the assembly of GJs in the saccule probably accounts for the death of saccular hair cells (Fig. 4H).

DISCUSSION

The results of this study show extensive co-expression of Cx26 and Cx30 in both the sensory and nonsensory epithelia of the saccule, utricle, and ampulla. Our Cx26 immunolabeling patterns are consistent with previous reports of Cx26 expression in the vestibular organs obtained with either immunostaining (Kikuchi et al., 1994) or electron microscopy examinations (Mulroy et al., 1993; Forge et al., 2003). In addition, we showed for the first time the extensive Cx30 immunoreactivity in the vestibular sensory organs and its co-localization with Cx26 in most GJ plaques (Figs. 1, 2). It is known that hybrid GJs consisting of Cx26 and Cx30 are the predominant molecular configuration for assembled GJs in the cochlear supporting cells and connective tissue cells (Lautermann et al., 1999; Ahmad et al., 2003; Forge et al., 2003). Therefore, our results indicate that intercellular GJ channels in both auditory and vestibular sensory regions are assembled mainly from Cx subunits consisting of Cx26 and Cx30.

We next examined functional requirements of the two Cxs for the survival of vestibular hair cells by using $Cx30^{-/-}$ mice (Teubner et al., 2003) and BAC^{Cx26};$Cx30^{-/-}$ mice (Ahmad et al., 2007). Our data demonstrate that, although the early development of vestibular hair cells in the saccule of the $Cx30^{-/-}$ mice was not affected, these cells degenerated similar to the cochlear hair cells later in development (Fig. 4H) (Ahmad et al., 2007; Teubner et al., 2003). In sharp contrast, vestibular hair cells in the utricle and ampulla were not appreciably affected by the lack of Cx30 (Fig. 4B,E). Survival of vestibular supporting cells may also be affected in the $Cx30^{-/-}$ mice because TUNEL-positive signals were detected in the supporting cell region (Fig. 7C), although the current study did not explicitly examine the relative time course of cell death in the hair cell and supporting cells regions. Our data, however, demonstrated for the first time that Cx30 is required for the survival of saccular hair cells. In contrast, the results also revealed that Cx30 is not required to maintain the survival of vestibular hair cells in the utricle and ampulla (Fig. 4B,E). Saccular hair cell death started with loss of hair bundles and was followed by disappearance of hair cell soma. This pattern of degeneration is consistent with a previous description of the pattern of vestibular hair cell death after ototoxic insults (Zheng et al., 1999). It is known that Cx26 is required for survival of cochlear hair cells (Cohen-Salmon et al., 2002), although it is not clear whether vestibular hair cells degenerate in the absence of Cx26 protein. Further work is needed to determine whether Cx26 is required for hair cell survival in any of the vestibular sensory organs.

The reason that vestibular hair cells degenerate only in the saccule of $Cx30^{-/-}$ mice, but not in the utricle and ampulla, is unclear. The utricle is connected to the endolymphatic duct by the utriculoendolymphatic valve. In contrast, the saccule is connected to the endolymphatic sac by the saccular duct and to the cochlea by the ductus reunions (Schuknecht, 1993). The ductus reunions provides a narrow pathway for cochlear fluid to mix with that in the saccule.

Conceivably, differences in fluid exchanges between the saccule and the other compartments of the vestibular end organs may be a factor contributing to heightened sensitivity of saccular hair cell loss. Dark cells, which are thought to play an important role in fluid homeostasis and which are metabolically active, are prevalent in the utricle and ampulae but not in the saccule of guinea pig (Ding et al., 1994) and pigmented mice (Ding, unpublished data). These cellular differences may also contribute to the increased vulnerability of the saccular hair cells in the $Cx30^{-/-}$ mice.

The requirements of both Cx26 and Cx30 for normal hearing are demonstrated by human homozygous mutation patients (Kelsell et al., 1997; del Castillo et al., 2002b) and their corresponding homozygous Cx deletion mouse models (Cohen-Salmon et al., 2002; Teubner et al., 2003). We did not observe any obvious signs of vestibular behavioral dysfunction in $Cx30^{-/-}$ mice. The nonsyndromic nature of $Cx30^{-/-}$ mutant mice could be explained by vestibular compensation, which is a well-known phenomenon confirmed in patients after unilateral removal of vestibular schwanoma (Wiegand et al., 1996). This interpretation is consistent with the fact that most Cx mutant patients do not show any clinical vestibular symptoms. However, our results also suggest that patients with Cx mutation should be carefully examined for signs of vestibular dysfunction associated with saccular degeneration. Recent results from humans with an enlarged vestibular aqueduct connecting the cochlea and saccule suggest that the vestibular myogenic response may be a useful tool for assessing saccular function in humans with $Cx30^{-/-}$ mutations (Sheykholeslami et al., 2004; Wang et al., 2006). In addition, the Tullio effect, whereby high-level sound stimulation induces eye movements and postural changes, could conceivably be used to test saccule dysfunction further in $Cx30^{-/-}$ mice (Dieterich et al., 1989).

Co-localization of Cx26 and Cx30 in most GJ plaques of the vestibular organs suggests that hybrid GJs are the major molecular configuration of these intercellular channels. Therefore, the functional requirements of Cx26 and/or Cx30 could be explained by at least two contrasting cellular mechanisms:

1. Cx30 is required as a component for the specific biophysical properties of hybrid GJ channels in the saccule. This hypothesis is consistent with findings for the GJ channels in the lens, where hybrid GJs are required for normal function (White, 2002). However, this hypothesis fails to account for the survival of hair cells in the utricle and ampulla (Fig. 4B,E).
2. Co-localization of Cx26 and Cx30 indicated that GJs in the saccule are normally produced from four copies of Cx genes (two Cx26 and two Cx30). Targeted deletion of Cx30 reduces the combined gene copy numbers to two, indicating that insufficient quantities of GJs may be produced in the saccule, which may ultimately result in hair cell degeneration.

In the $Cx30^{-/-}$;BAC^{Cx26} mice, our previously published results (Ahmad et al., 2007) indicated that the protein level of Cx26 was overexpressed in the liver and restored to the WT level in the cochlea. Although we did not specifically measure mRNA and protein levels in the vestibular sensory organs, increased gene transcription and translation by BAC transgenic expression are likely to cause increased production of Cx26 in the vestibular organs (Yang et al., 1997). The rescue results (Fig. 4C,F,I) obtained from BAC^{Cx26};$Cx30^{-/-}$ mice demonstrated that hybrid GJs consisting of Cx26 and Cx30 were not essential for survival of saccular vestibular hair cells. We therefore have defined a basic requirement for the molecular configuration of a major type of GJs for the survival of saccular hair cells. Similar to hair cells in the cochlea (Ahmad et al., 2007), insufficient quantity of GJs apparently underlie the death of vestibular hair cells. Our results, therefore, predict that a therapy based on a drug treatment that either increases translation or slows down the degradation of surviving Cx gene in the

hybrid GJ complex may be sufficient to rescue saccular hair cells from degeneration. Further experiments are needed to test this intriguing hypothesis.

Acknowledgements

The authors thank Dr. Philine Wangemann for providing valuable comments on the manuscript.

Grant sponsor: National Institutes of Health; Grant numbers: RO1-DC04709 and RO1-DC006483 (to X.L.) and R01 DC06630 (to R.S.); Grant sponsor: Woodruff Foundation (to X.L.); Grant sponsor: German Research Association (to K.W.); Grant sponsor: Fritz Thyssen Foundation (to K.W.); Grant sponsor: the National Organization for Hearing Research (to W.T.); Grant sponsor: the Deafness Research Foundation (to W.T.); Grant sponsor: the Hebei Provincial Government of China (to Q.Y.).

LITERATURE CITED

Ahmad S, Chen S, Sun J, Lin X. Connexins 26 and 30 are co-assembled to form gap junctions in the cochlea of mice. Biochem Biophys Res Commun 2003;307:362–368. [PubMed: 12859965]

Ahmad S, Tang W, Chang Q, Qu Y, Hibshman J, Li Y, Sohl G, Willecke K, Chen P, Lin X. Restoration of connexin26 protein level in the cochlea completely rescues hearing in a mouse model of human connexin30-linked deafness. Proc Natl Acad Sci U S A 2007;104:1337–1341. [PubMed: 17227867]

Cohen-Salmon M, Ott T, Michel V, Hardelin JP, Perfettini I, Eybalin M, Wu T, Marcus DC, Wangemann P, Willecke K, Petit C. Targeted ablation of connexin26 in the inner ear epithelial gap junction network causes hearing impairment and cell death. Curr Biol 2002;12:1106–1111. [PubMed: 12121617]

del Castillo I, Villamar M, Moreno-Pelayo MA, del Castillo FJ, Alvarez A, Telleria D, Menendez I, Moreno F. A deletion involving the connexin 30 gene in nonsyndromic hearing impairment. N Engl J Med 2002a;346:243–249. [PubMed: 11807148]

del Castillo I, Villamar M, Moreno-Pelayo MA, del Castillo FJ, Alvarez A, Telleria D, Menendez I, Moreno F. A deletion involving the connexin 30 gene in nonsyndromic hearing impairment. N Engl J Med 2002b;346:243–249. [PubMed: 11807148]

Dieterich M, Brandt T, Fries W. Otolith function in man. Results from a case of otolith Tullio phenomenon. Brain 1989;112:1377–1392. [PubMed: 2804618]

Ding D, Huangfu M, Jin X. The relations between vestibular anatomic characteristics and experimental endolymphatic hydrops. Acta Otolarygol China 1994;8:1–2.

Forge A, Becker D, Casalotti S, Edwards J, Marziano N, Nevill G. Gap junctions in the inner ear: comparison of distribution patterns in different vertebrates and assessement of connexin composition in mammals. J Comp Neurol 2003;467:207–231. [PubMed: 14595769]

Gale JE, Meyers JR, Periasamy A, Corwin JT. Survival of bundleless hair cells and subsequent bundle replacement in the bullfrog's saccule. J Neurobiol 2002;50:81–92. [PubMed: 11793356]

Gerido DA, White TW. Connexin disorders of the ear, skin, and lens. Biochim Biophys Acta 2004;1662:159–170. [PubMed: 15033586]

Hasson T, Gillespie P, Garcia J, MacDonald R, Zhao Y, Yee A, Mooseker M, Corey D. Unconventional myosins in inner-ear sensory epithelia. J Cell Biol 1997;137:1287–1307. [PubMed: 9182663]

Kelsell DP, Dunlop J, Stevens HP, Lench NJ, Liang JN, Parry G, Mueller RF, Leigh IM. Connexin 26 mutations in hereditary nonsyndromic sensorineural deafness. Nature 1997;387:80–83. [PubMed: 9139825]

Kikuchi T, Adams JC, Paul DL, Kimura RS. Gap junction systems in the rat vestibular labyrinth: immunohistochemical and ultrastructural analysis. Acta Otolaryngol 1994;114:520–528. [PubMed: 7825434]

Lautermann J, Frank HG, Jahnke K, Traub O, Winterhager E. Developmental expression patterns of connexin26 and -30 in the rat cochlea. Dev Genet 1999;25:306–311. [PubMed: 10570462]

Mulroy MJ, Dempewolf SA, Curtis S, Iida HC. Gap junctional connections between hair cells, supporting cells and nerves in a vestibular organ. Hear Res 1993;71:98–105. [PubMed: 8113149]

Schuknecht, HF. Pathology of the ear. Philadelphia: Lea & Febiger; 1993.

Sheykholeslami K, Schmerber S, Habiby Kermany M, Kaga K. Vestibular-evoked myogenic potentials in three patients with large vestibular aqueduct. Hear Res 2004;190:161–168. [PubMed: 15051138]

Sun J, Ahmad S, Chen S, Tang W, Zhang Y, Chen P, Lin X. Cochlear gap junctions coassembled from Cx26 and 30 show faster intercellular Ca2+ signaling than homomeric counterparts. Am J Physiol Cell Physiol 2005;288:C613–623. [PubMed: 15692151]

Teubner B, Michel V, Pesch J, Lautermann J, Cohen-Salmon M, Sohl G, Jahnke K, Winterhager E, Herberhold C, Hardelin JP, Petit C, Willecke K. Connexin30 (Gjb6)-deficiency causes severe hearing impairment and lack of endocochlear potential. Hum Mol Genet 2003;12:13–21. [PubMed: 12490528]

Thonnissen E, Rabionet R, Arbones ML, Estivill X, Willecke K, Ott T. Human connexin26 (GJB2) deafness mutations affect the function of gap junction channels at different levels of protein expression. Hum Genet 2002;111:190–197. [PubMed: 12189493]

Wang YP, Hsu WC, Young YH. Vestibular evoked myogenic potentials in acute acoustic trauma. Otol Neurotol 2006;27:956–961. [PubMed: 17006346]

White TW. Unique and redundant connexin contributions to lens development. Science 2002;295:319–320. [PubMed: 11786642]

Wiegand DA, Ojemann RG, Fickel V. Surgical treatment of acoustic neuroma (vestibular schwannoma) in the United States: report from the Acoustic Neuroma Registry. Laryngoscope 1996;106:58–66. [PubMed: 8544629]

Yang XW, Model P, Heintz N. Homologous recombination based modification in *Escherichia coli* and germline transmission in transgenic mice of a bacterial artificial chromosome. Nat Biotechnol 1997;15:859–865. [PubMed: 9306400]

Zheng JL, Keller G, Gao WQ. Immunocytochemical and morphological evidence for intracellular self-repair as an important contributor to mammalian hair cell recovery. J Neurosci 1999;19:2161–2170. [PubMed: 10066269]

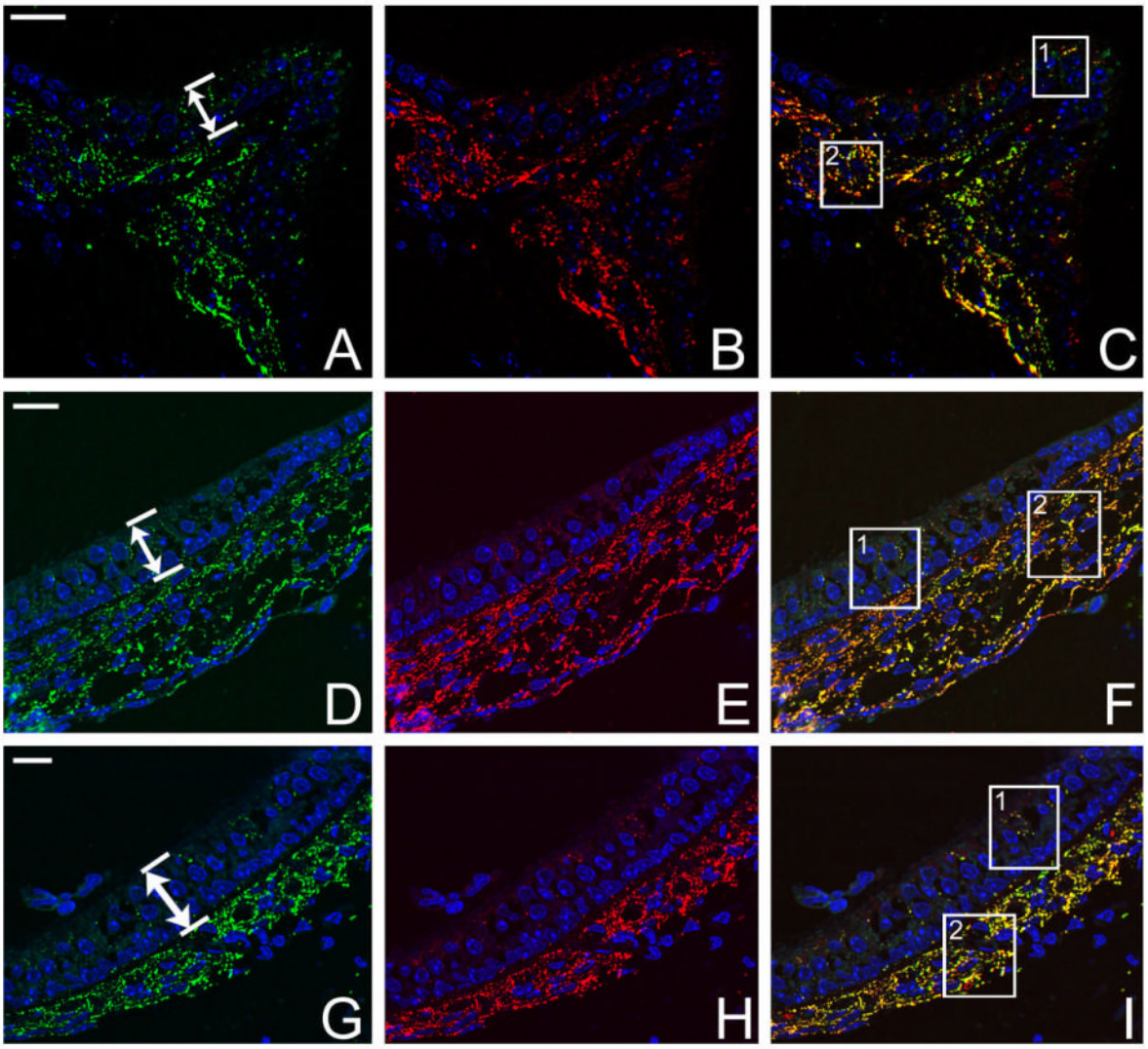

Fig. 1.

Results of double immunolabeling of Cx26 (red) and Cx30 (green) in semithin sections of vestibular sensory organs of WT adult mice. Cryosections were counterstained with DAPI (blue) to reveal cell nuclei. **A,D,G:** Immunolabeling of Cx30 in ampulla, saccule, and utricle, respectively. **B,E,H:** Same sections as in A, D, and G double immunolabeled with Cx26 in ampulla, saccule, and utricle, respectively. **C,F,I:** Overlapped images of double immunolabeling in the three vestibular sensory regions. Double-headed arrows in A, D, and G indicate the bottom and top borders of the vestibular sensory epithelia. Boxed areas are shown in Figure 2 at higher magnification. Scale bar = ~20 μm in A (applies to A–C); D (applies to D–F); G (applies to G–I).

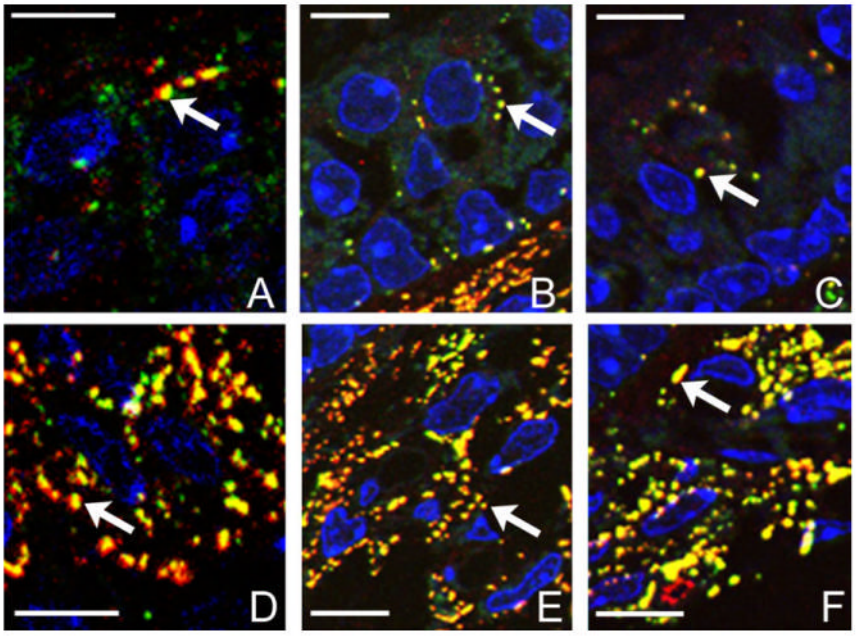

Fig. 2.

Enlarged images showing details of boxed areas in Figure 1C, F, and I. **A–C:** Boxed areas labeled with the number 1. **D–F:** Areas labeled with the number 2. Arrows point to examples of individual puncta co-labeled with Cx26 and Cx30, suspected to be hybrid GJ plaques. Scale bar = ~10 μm in A–F.

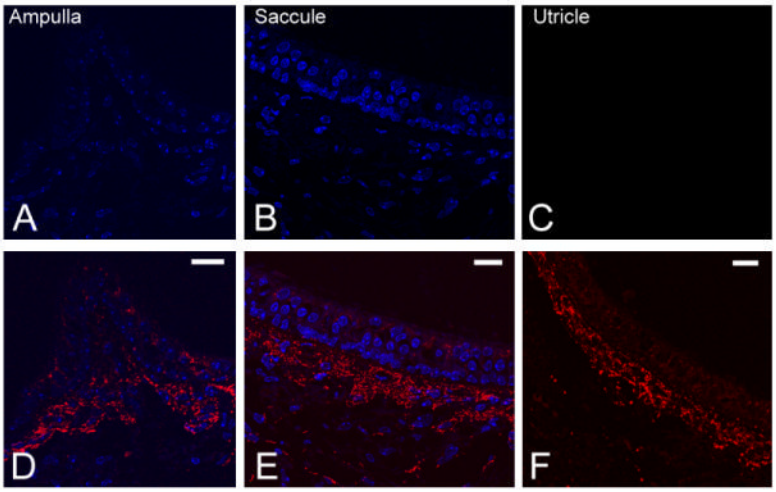

Fig. 3.

Immunolabeling data showing patterns of Cx30 (**A–C**) and Cx26 (**D–F**) expressions in the ampulla, saccule, and utricle of adult $Cx30^{-/-}$ mice. Sections were counterstained with DAPI (blue) to reveal locations of cell nuclei. Scale bar = ~20 μm in D (applies to A,D); E (applies to B,E); F (applies to C,F).

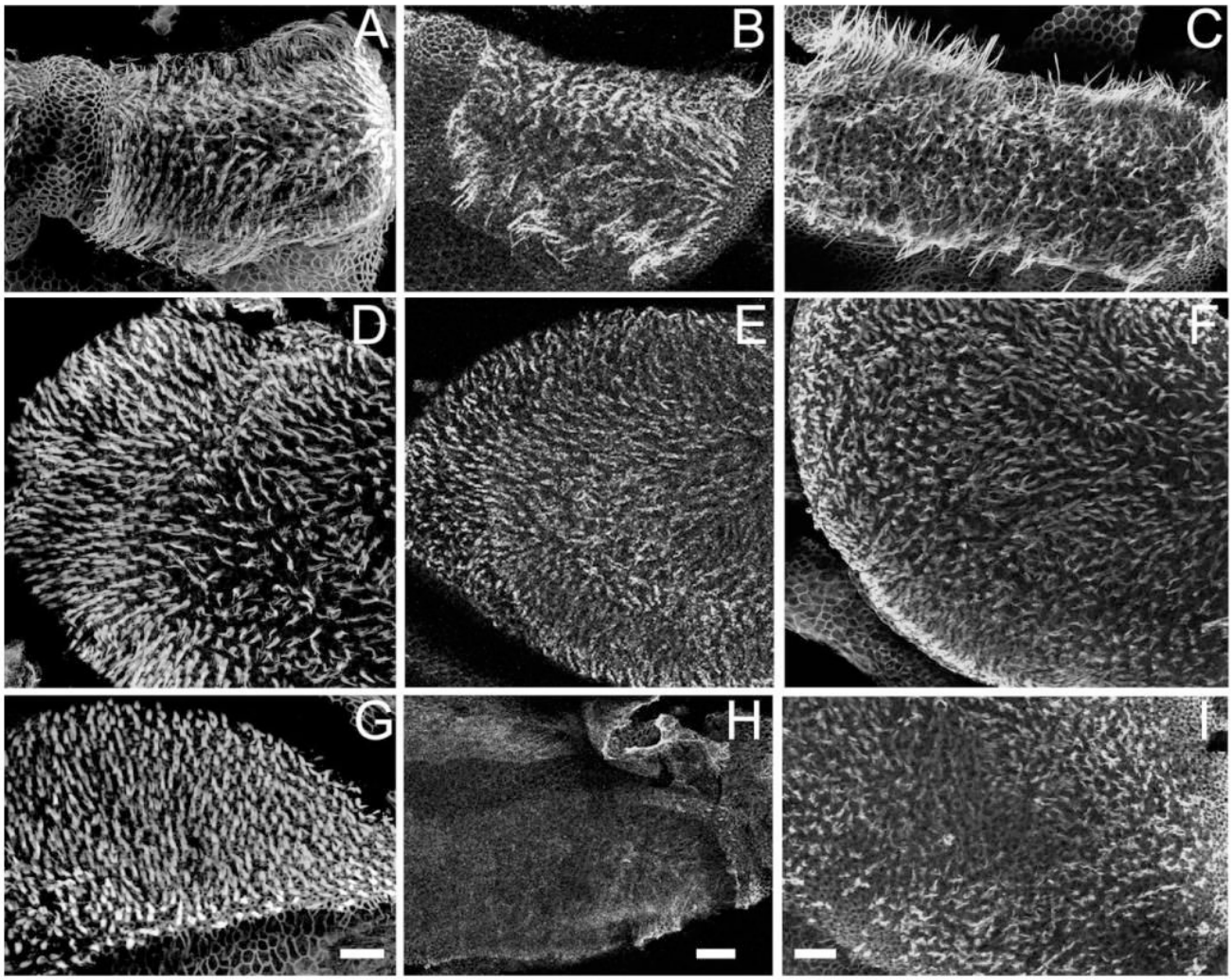

Fig. 4.

Confocal images comparing morphology of hair bundles in the three vestibular sensory regions of WT, $Cx30^{-/-}$, and BAC^{Cx26}; $Cx30^{-/-}$ (rescued) mice. Phalloidin-labeled hair bundles observed in ampulla (**A–C**), utricle (**D–F**), and saccule (**G–I**) are shown. Results obtained from the three vestibular sensory regions of WT (A,D,G), $Cx30^{-/-}$ (B,E,H), and BAC^{Cx26};$Cx30^{-/-}$ (C,F,I) mice are shown in each column. Adult (1–2-month-old) mice were used. Scale bar = ~100 μm in G (applies to A,D,G); H (applies to B,E,H); I (applies to C,F,I).

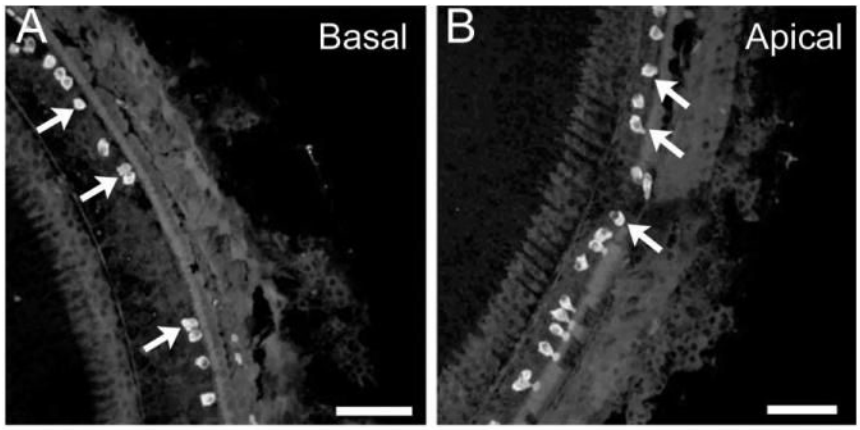

Fig. 5.

Myosin7-labeled cochlear hair cells observed in the basal (**A**) and apical (**B**) turns of $Cx30^{-/-}$ mice. Arrows point to examples of remaining inner hair cells. Adult (1–2-month-old) mice were used. Scale bar = ~100 μm in A,B.

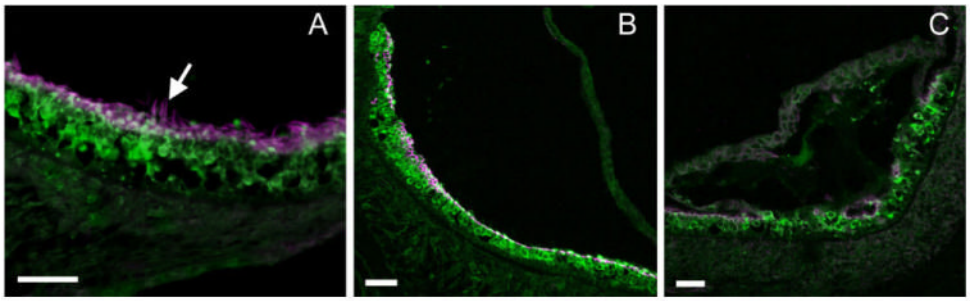

Fig. 6.

Double immunolabeling of hair cell soma (green) and stereocilia (magenta) in cross sections of the saccule of $Cx30^{-/-}$ mice. Arrow points to hair bundles of hair cells. Results obtained from P4 (**A**), P14 (**B**), and P30 (**C**) mice are given. Scale bar = ~100 μm in A–C.

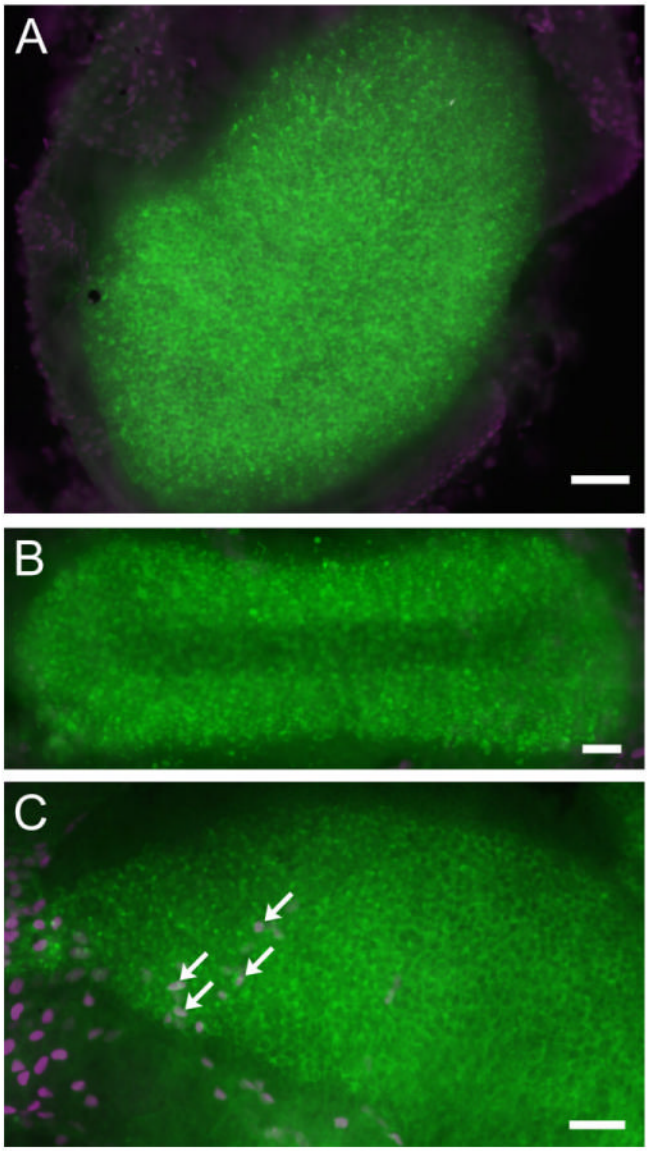

Fig. 7.

A-C: TUNEL labeling (magenta) of the three vestibular sensory regions obtained from $Cx30^{-/-}$ mice (~1 month old). Soma of hair cells was labeled with an antibody against myosin7 (in green). Arrows in C point to examples of TUNEL-positive hair cells in the saccule. Scale bar = ~50 μm in A-C.